THE DUAL POLARIZATION GNSS-R INTERFERENCE PATTERN TECHNIQUE

A. Alonso-Arroyo[1], *A.Camps*[1], *A. Monerris*[2], *C. Rüdiger* [2], *J.P. Walker*[2], *G.Forte* [1], *D. Pascual*[1], *H. Park*[1], *R. Onrubia*[1]

[1]Remote Sensing Laboratory, Department of Signal Theory and Communications,
Universitat Politècnica de Catalunya Barcelona-Tech and IEEC/UPC UPC
C/Jordi Girona 1-3, Campus Nord D3, 08034 Barcelona, Spain
e-mail: alberto.alonso.arroyo@tsc.upc.edu
[2]Department of Civil Engineering, Monash University,
Wellington Rd, Clayton, VIC 3800, Australia
e-mail: sandra.monerris-belda@monash.edu

ABSTRACT

Since 2003 several field experiments using Global Navigation Satellite Systems (GNSS)-Reflectometry (GNSS-R) have demonstrated the feasibility of retrieving Soil Moisture (SM) from GNSS-R observations. Different techniques such as the power difference between direct and reflected signals, the Signal to Noise Ratio (SNR)-analysis method, the Interference Pattern Technique (IPT) or the Interferometric Complex Field (ICF) have been used. The conventional IPT was first proposed in 2008, and consisted on forcing a single multipath using a vertically polarized GNSS antenna with a rotationally symmetric pattern pointing to the horizon. In this work the conventional IPT is extended to dual-polarization, horizontal (H-pol) and vertical (V-pol), in attempt to increase the accuracy in the SM retrievals. In this case, the Brewster angle is estimated from the phase difference between the H- and V-Pol interference patterns. The use of dual-polarization measurements is not sensitive to surface roughness and it is more precise in the determination of the Brewster angle position. Results from a field experiment at the Yanco site, New South Wales, Australia, are shown to demonstrate the concepts proposed in this work.

Index Terms— GNSS-R, Soil Moisture, Interference Pattern Technique, Dual-Polarization, Dielectric constant.

These activities have been sponsored by the Spanish Ministry of Science and Innovation, "AROSA-Advanced Radio Ocultations and Scatterometry Applications using GNSS and other opportunity signals", code AYA2011-29183-C02-01/ESP and a Monash University Faculty of Engineering Seed grant 2013. The authors acknowledge the support by ACROSS (Advanced Remote Sensing Ground-Truth Demo and Test Facilities) and TERENO (Terrestrial Environmental Observatories) funded by the German Helmholtz-Association; the CosmOz network and the funding provided by the Commonwealth Scientific and Industrial Research Organisation; and the OzNet hydrological monitoring network. The authors would also like to thank Frank Winston for his help in the installation and maintenance of P-SMIGOL at the experiment site.

1. INTRODUCTION

GNSS-R has been widely used for the retrieval of SM at local and medium scales. In 2003, the observation of the power difference between direct and reflected GNSS signals at Right Hand Circular Polarization (RHCP), Left Hand Circular Polarization (LHCP), H- and V-pol from a ground-based platform was compared to the in-situ SM content at 6 cm depth [1]. Correlation between SNR and SM was found for SM contents larger than 20% [1]. The ratio of the H- and V-pol estimated reflectivity should theoretically cancel surface roughness attenuation preserving the dielectric constant information [2]. Results from the SMEX02 experiment confirmed that, under airborne conditions and using a zenith-looking RHCP antenna and a nadir-looking LHCP antenna, the reflected GNSS signal power increases with SM content [3, 4]. The ICF [5], a time series of the ratio between the direct and reflected waveform peaks, was later used for the determination of the surface reflection coefficient. From the estimated averaged reflection coefficient, the SM can be retrieved [6].

Another GNSS-R approach followed by different researchers to estimate SM is the IPT. The feasibility of sensing the complex dielectric constant of soil by Global Positioning System (GPS) multi-path observations due to the Brewster angle position was first assessed in 1998 [7]. The IPT technique has also been used to determine SM and vegetation parameters using a V-pol antenna with a rotationally symmetric antenna pattern [8, 9]. A similar approach has been followed using GPS geodetic antennas, which is also known as SNR-analysis method [10, 11]. The SNR-analysis method acquires the reflected signals from the sidelobes of the antenna pattern. As a geodetic antenna is purely RHCP, the information provided by the Brewster angle, which occurs only at V-Pol, is masked and cannot be used. Other observables such as the phase difference between consecutive interference patterns can be used to determine relative SM changes.

This work extends the conventional IPT proposed in [8,9] to dual-polarization observations, H-pol and V-pol. In Section 2 the theoretical model of the technique is presented. In Section 3 simulations using that model are shown. In Section 4 preliminary results from a field campaign are presented. Finally, Section 5 presents the main conclusions of this work.

2. THEORETICAL REVIEW

The IPT consists of the coherent addition of the direct and the reflected GNSS signals collected with a linearly polarized antenna pointing to the horizon. Taking into account that direct and reflected GNSS signals are circularly polarized, and that the reflected signal polarization may change from LHCP to RHCP for very low grazing angles, the use of linearly polarized antennas exhibits several advantages. First, the information provided by the Brewster angle can be used as it only occurs at V-pol. Second, the polarization dependency of the reflected signal on the incidence angle is nearly lost along the antenna beamwidth, as each linear polarization is sensitive to one of the circular polarization components. Third, a linear dual-polarization antenna with a high cross-polar ratio allows the acquisition of both H- and V-pol interference patterns at the same time. If this linearly polarized antenna has a rotationally symmetric pattern, the theoretical IPT model can be expressed by Eqn. (1).

$$P_R \propto |E_i + E_r|^2 = F_n(\theta_{elev}) \cdot |E_{0_i}|^2 \cdot \\ \cdot |1 + |R_q(\theta_{elev}, \varepsilon_r)| \cdot e^{j(\Delta\phi + \phi_{R_q}(\theta_{elev}, \varepsilon_r))}|^2, \quad (1)$$

where: P_R is the instantaneous received/interference power, E_i and E_r are the incident and reflected fields respectively, $F_n(\theta_{elev})$ is the antenna radiation pattern, E_{0_i} the amplitude of the incident electric field, $|R_q(\theta_{elev}, \varepsilon_r)|$ the absolute value of the Fresnel reflection coefficient at q polarization, $\phi_{R_q}(\theta_{elev}, \varepsilon_r)$ the phase of the Fresnel reflection coefficient at q polarization, $\Delta\phi = \frac{4\pi}{\lambda} h \sin(\theta_{elev})$ the phase difference due to the different electrical path between direct and scattered electro-magnetic (EM) waves, h the height of the receiving antenna, λ is the EM wavelength ($\sim$ 19 cm), and ε_r the soil surface dielectric constant.

From Eqn. (1) it is seen that the only components that depend on the soil dielectric constant and consequently on the SM are the Fresnel reflection coefficient magnitude and phase. To assess the impact of SM on the interference pattern, simulations using the dielectric constant model in [12] and a two-layer model of the Fresnel reflection coefficients (Eqns. (2)-(3)) were performed:

$$R_{h_{1,2}} = \frac{\sqrt{1 - sin^2(\theta_{inc})} - \sqrt{\varepsilon_{r_2} - sin^2(\theta_{inc})}}{\sqrt{1 - sin^2(\theta_{inc})} + \sqrt{\varepsilon_{r_2} - sin^2(\theta_{inc})}}, \quad (2)$$

$$R_{v_{1,2}} = \frac{\varepsilon_{r_2} \cdot \sqrt{1 - sin^2(\theta_{inc})} - \sqrt{\varepsilon_{r_2} - sin^2(\theta_{inc})}}{\varepsilon_{r_2} \cdot \sqrt{1 - sin^2(\theta_{inc})} + \sqrt{\varepsilon_{r_2} - sin^2(\theta_{inc})}}, \quad (3)$$

To take into account surface roughness, Eqn. (4) has been used [13].

$$\Gamma_q = |R_{q_{1,2}}|^2 \cdot e^{-4 \cdot k^2 \cdot \sigma_h{}^2 \cdot \cos^2(\theta_{inc})}, \quad (4)$$

where: ε_{r_2} is the dielectric constant of the soil layer, θ_{inc} the incidence angle, q the polarization (H-pol or V-pol), $k = \frac{2\pi}{\lambda}$, and σ_h the surface *rms* height.

3. SIMULATIONS

In this section, simulations of different reflection coefficients and interference patterns are shown for different SM contents. On one hand, Fig. 1a shows the reflectivity curves for H-pol (diamonds) and for V-pol (squares) for different SM values and a specific soil composition. H-pol reflectivity decreases monotonically with the elevation angle. It is straightforward to identify the Brewster angle position at V-pol as it corresponds to the minimum amplitude point. On the other hand, Fig. 1b shows the phase of the reflection coefficient at H-pol (diamonds) and V-pol (squares) for the same conditions than Fig. 1a. The phase of the reflection coefficient at H-pol is very close to 180° independently from SM conditions. At V-pol, the behavior of the phase is different and it varies from 180° to 0° in a sharp transition. The steepness of this transition depends on the SM conditions and soil texture. Analyzing and comparing both sub-figures on Fig. 1 it is observed that the minimum amplitude point at Fig. 1a corresponds to the 90° phase shift of Fig. 1b. This means that when the phase difference between H-pol and V-pol reflection coefficients is 90°, the Brewster angle is found [14].

This fact observed on the reflection coefficients is seen on the interference patterns at H- and V-pol as both are in phase when the reflection coefficient phase is the same, whereas both are in counter-phase when the reflection coefficient phase is opposite. Figure 2 shows two simulated interference patterns for 10% and 30% SM content. In there, it is straightforward to identify the notch position, and when H-pol and V-pol interference patterns are in phase or in counter-phase. These helps to increase the estimation accuracy of the Brewster angle position.

4. EXPERIMENTAL RESULTS

In July 2013 a field experiment was conducted at the Yanco site, New South Wales, Australia, to test this theory. An upgraded version of the SMIGOL instrument in [8] was used. The main difference between these two instruments is the addition of a dual-polarization antenna (H-pol and V-pol) with a high cross-polar ratio to avoid cross-polar contamination, and

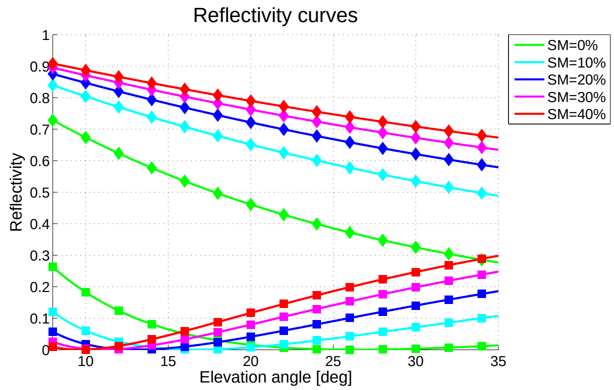

(a) Amplitude curves.

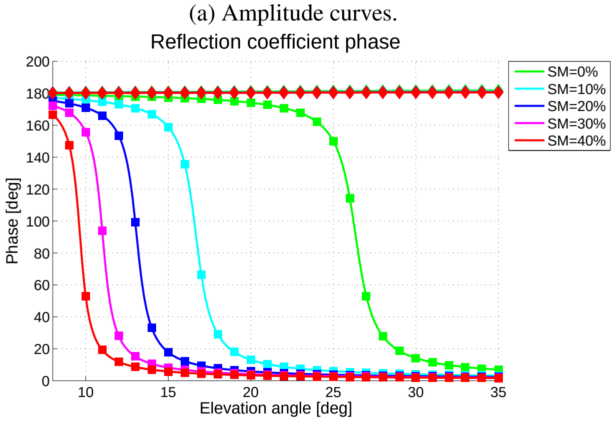

(b) Phase curves.

Fig. 1: Reflection coefficient plots as a function of the SM: diamonds indicate H-pol, squares indicate V-pol. Adapted from [14].

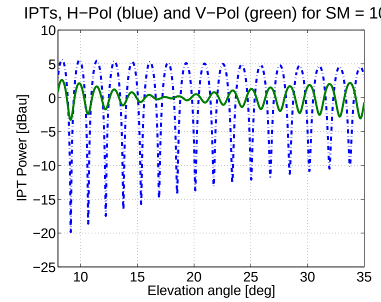

(a) 10% SM content.

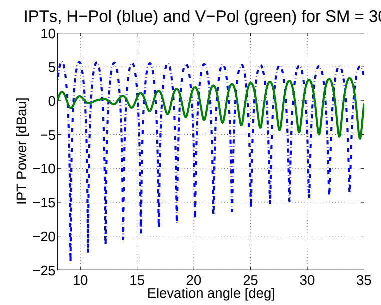

(b) 30% SM content.

Fig. 2: Interference patterns simulated for two different SM values: (a) 10% and (b) 30%. H-pol (blue dashed), V-Pol (green). Adapted from [14].

the addition of two receiving chains, one for each polarization.

Figure 3 shows an interference pattern measured during the field campaign. The H-pol is marked in red and the V-pol in blue. It is seen that the oscillation amplitude in H-pol is larger than in V-pol due to the larger reflection coefficient. At V-pol, it is quite difficult to identify where the Brewster angle is, as there is a region with the same oscillation amplitude. The phase observation algorithm helps to determine the position of the Brewster angle more accurately.

A 15-day dataset, from July 16^{th} to July 31^{st}, has been processed and compared with ground-truth data in order to validate the proposed theoretical developments. Results are represented in Fig. 4, which shows that the variation of the SM retrieved using the proposed algorithm is smoother than when looking to the minimum amplitude position only, which matches with the ground-truth information.

5. CONCLUSIONS AND FUTURE WORK

This work has extended the conventional IPT to dual-pol observations. By observing the relative phase difference between the H- and V-pol interference patterns it is possible to track the phase difference between both reflection coefficients. When this phase difference is 90° the Brewster angle position is found. This algorithm helps to identify the minimum amplitude point in situations when the oscillation frequency of the interference pattern is low, i.e. when the instrument is at a low height ($h < 2$ m). As the reflection coefficient is larger at H-pol than at V-pol, and its variations are larger depending on the SM content, the next step is to relate the Brewster angle position with SM retrievals using the H-pol interference patterns.

6. REFERENCES

[1] V. Zavorotny, D. Masters, A. Gasiewski, B. Bartram, S. Katzberg, P. Axelrad, and R. Zamora, "Seasonal polarimetric measurements of soil moisture using tower-based GPS bistatic radar," in *IGARSS 2003. 2003 IEEE Int. Geosci. Remote Sens. Symp. Proc. (IEEE Cat. No.03CH37477)*. vol. 2, pp. 781–783, IEEE.

[2] V.U. Zavorotny and A.G. Voronovich, "Bistatic GPS signal re-

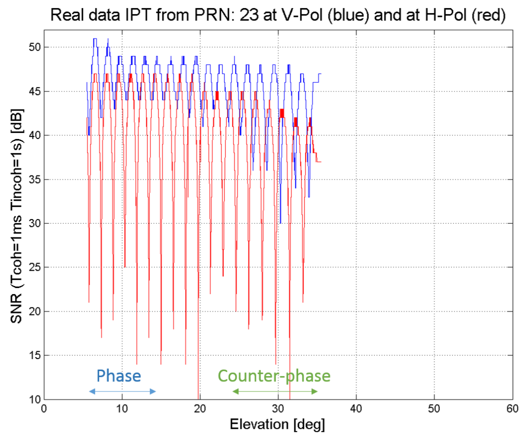

Fig. 3: Experimental interference pattern from satellite 23. H-Pol (red), V-Pol (blue).

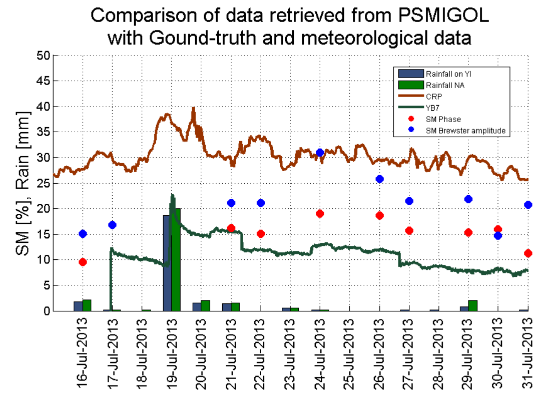

Fig. 4: Inter-comparison of soil moisture and ground-truth retrievals. Grey and green bars represent rainfalls. The brown line represents the data from the CRP. The green line shows the data from the SDI-12 SM probe. Red dots represent the mean SM retrieved from phase measurements using the PSMIGOL instrument. Blue dots represent the mean SM retrieved from Brewster angle position, also from PSMIGOL.

flections at various polarizations from rough land surface with moisture content," in *IGARSS 2000. IEEE 2000 Int. Geosci. Remote Sens. Symp. Tak. Pulse Planet Role Remote Sens. Manag. Environ. Proc. (Cat. No.00CH37120)*. 2000, vol. 7, pp. 2852–2854, IEEE.

[3] Dallas Masters, Penina Axelrad, and Stephen J. Katzberg, "Initial results of land-reflected GPS bistatic radar measurements in SMEX02," *Remote Sens. Environ.*, vol. 92, no. 4, pp. 507–520, Sept. 2004.

[4] Stephen J. Katzberg, Omar Torres, Michael S. Grant, and Dallas Masters, "Utilizing calibrated GPS reflected signals to estimate soil reflectivity and dielectric constant: Results from SMEX02," *Remote Sens. Environ.*, vol. 100, no. 1, pp. 17–28, Jan. 2006.

[5] G. Ruffini and F. Soulat, "On the GNSS-R Interferometric Complex Field Coherence Time," June 2004.

[6] Alejandro Egido, Giulio Ruffini, Marco Caparrini, Cristina Martin, Esteve Farres, and Xavier Banque, "Soil Moisture Monitorization Using GNSS Reflected Signals," p. 7, May 2008.

[7] A. Kavak, W.J. Vogel, and Guanghan Xu, "Using GPS to measure ground complex permittivity," *Electron. Lett.*, vol. 34, no. 3, pp. 254, 1998.

[8] N. Rodriguez-Alvarez, X. Bosch-Lluis, A. Camps, M. Vall-llossera, E. Valencia, J.F. Marchan-Hernandez, and I. Ramos-Perez, "Soil Moisture Retrieval Using GNSS-R Techniques: Experimental Results Over a Bare Soil Field," *IEEE Trans. Geosci. Remote Sens.*, vol. 47, no. 11, pp. 3616–3624, Nov. 2009.

[9] Nereida Rodriguez-Alvarez, Adriano Camps, Mercè Vall-llossera, Xavier Bosch-Lluis, Alessandra Monerris, Isaac Ramos-Perez, Enric Valencia, Juan Fernando Marchan-Hernandez, Jose Martinez-Fernandez, Guido Baroncini-Turricchia, Carlos Perez-Gutierrez, and Nilda Sanchez, "Land Geophysical Parameters Retrieval Using the Interference Pattern GNSS-R Technique," *IEEE Trans. Geosci. Remote Sens.*, vol. 49, no. 1, pp. 71–84, Jan. 2011.

[10] Kristine M. Larson, Eric E. Small, Ethan D. Gutmann, Andria L. Bilich, John J. Braun, and Valery U. Zavorotny, "Use of GPS receivers as a soil moisture network for water cycle studies," *Geophys. Res. Lett.*, vol. 35, no. 24, pp. L24405, Dec. 2008.

[11] Valery U. Zavorotny, Kristine M. Larson, John J. Braun, Eric E. Small, Ethan D. Gutmann, and Andria L. Bilich, "A Physical Model for GPS Multipath Caused by Land Reflections: Toward Bare Soil Moisture Retrievals," *IEEE J. Sel. Top. Appl. Earth Obs. Remote Sens.*, vol. 3, no. 1, pp. 91–99, Mar. 2010.

[12] James R. Wang and Thomas J. Schmugge, "An Empirical Model for the Complex Dielectric Permittivity of Soils as a Function of Water Content," *IEEE Trans. Geosci. Remote Sens.*, vol. GE-18, no. 4, pp. 288–295, Oct. 1980.

[13] P. Beckmann; A. Spizzichino, *The scattering of electromagnetic waves from rough surfaces*, Artech Print on Demand, 1987.

[14] A. Alonso-Arroyo, A. Camps, A. Aguasca, G. Forte, A. Monerris, C. Rudiger, J. P. Walker, H. Park, D. Pascual, and R. Onrubia, "Improving the Accuracy of Soil Moisture Retrievals Using the Phase Difference of the Dual-Polarization GNSS-R Interference Patterns," *IEEE Geosci. Remote Sens. Lett.*, pp. 1–5, 2014.